Influence of non-solvent chemistry on polybenzimidazole hollow fiber membrane preparation

Dahe, Ganpat
Singh, Rajinder Pal
Dudeck, Kevin Wade
Yang, Dali
Berchtold, Kathryn A.

To be published in: Journal of Membrane Science

DOI to publisher's version: 10.1016/j.memsci.2019.02.001

Author's Accepted Manuscript

www.elsevier.com/locate/memsci

Influence of Non-solvent Chemistry on Polybenzimidazole Hollow Fiber Membrane Preparation

Ganpat J. Dahe, Rajinder P. Singh, Kevin W. Dudeck, Dali Yang, Kathryn A. Berchtold

PII: S0376-7388(18)31449-2
DOI: https://doi.org/10.1016/j.memsci.2019.02.001
Reference: MEMSCI16826

To appear in: *Journal of Membrane Science*

Received date: 29 May 2018
Revised date: 3 October 2018
Accepted date: 2 February 2019

Cite this article as: Ganpat J. Dahe, Rajinder P. Singh, Kevin W. Dudeck, Dali Yang and Kathryn A. Berchtold, Influence of Non-solvent Chemistry on Polybenzimidazole Hollow Fiber Membrane Preparation, *Journal of Membrane Science,* https://doi.org/10.1016/j.memsci.2019.02.001

Influence of Non-solvent Chemistry on Polybenzimidazole Hollow Fiber Membrane Preparation

Ganpat J. Dahe[1], Rajinder P. Singh[1,*], Kevin W. Dudeck[1], Dali Yang[2], Kathryn A. Berchtold[1,*]

[1]Carbon Capture and Separations for Energy Applications (CaSEA) Labs

Materials Physics and Applications Division, [2]Materials Science and Technology Division Los Alamos National Laboratory, Los Alamos, NM 87545

rsingh@lanl.gov

berchtold@lanl.gov

[*]Corresponding Authors:

Abstract

Polybenzimidazole membrane materials have attractive H_2/CO_2 separation characteristics and high thermo-chemical stability for elevated temperature synthesis (syn) gas separations. The development of PBI membranes with a thin defect-free selective layer and porous support morphology is vital to achieving industrially attractive separation performance. This work is focused on developing a fundamental understanding of the liquid-liquid demixing-based phase inversion process for asymmetric PBI hollow fiber membrane (HFM) formation. The development of industrially attractive HFMs is a challenging process due to the complex interplay between phase equilibria, phase inversion kinetics, and interfacial mass transfer that exist during the liquid-liquid demixing process. Numerous parameters including the dope, bore, and outer coagulant chemistries and compositions significantly influence the HFM morphologies produced. Here, a systematic study is conducted to investigate the phase inversion process parameters including the roles of the non-solvent solubility and diffusivity parameters with respect to the solvent and PBI on the phase inversion process. Furthermore, the influence of dope, bore and coagulant chemistries and compositions on PBI HFM morphology are investigated. The fabricated PBI HFMs are evaluated for their ideal H_2 and CO_2 permeance and H_2/CO_2 selectivity at 250 °C to benchmark their separation performance.

Keywords: Polybenzimidazole, hollow fiber membrane fabrication, non-solvent selection, selective layer optimization, phase inversion, syngas separation, carbon capture, IGCC

1 Introduction

Polybenzimidazole (PBI)-based materials for membrane separation have received major attention due to their exceptional thermal and chemical stability in extremely challenging process environments. These properties have attracted many researchers to investigate PBI-based materials for applications with operating conditions well outside the typical realm of organic materials. These applications include fuel cells [1], reverse osmosis [2], forward osmosis [3], nanofiltration [4], organic solvent nanofiltration [5, 6], and gas separations [7, 8].

PBI-based materials are attractive for elevated temperature synthesis gas (syngas) separations owing to aforementioned stability characteristics; of particular interest in their high degradation temperatures approaching 500 °C. Syngas, which is a mixture predominantly comprising H_2, CO, CO_2 and steam, is produced at high temperature and pressure in an integrated gasification combined cycle (IGCC) process using hydrocarbon fuels including coal. The presence of H_2S, steam, and high temperatures makes hydrocarbon fuel derived syngas separations technically and economically challenging. Current benchmark processes for syngas separations operate at ambient or near ambient temperatures and low pressure resulting in significant energy penalties [9, 10]. Our previous work demonstrates both the utility of PBI membranes in syngas process environments and operating conditions and their commercially attractive H_2/CO_2 selectivity [7, 11]. The elevated temperature gas separation characteristics of PBI membranes presents energy efficient process integration opportunities, which are not readily available with the industry standard CO_2 separation methods.

In an IGCC process, large volumes of syngas are produced, which requires a high throughput membrane platform such as the hollow fiber membrane (HFM) platform. Furthermore, the H_2 permeability of commercially available PBI materials mandates thin selective layers to achieve industrially attractive and economically viable throughputs [7]. The development of industrially attractive PBI HFMs having thin selective and porous support layers is a challenging process due to the complex interplay between phase equilibria, phase inversion kinetics, and interfacial mass transfer that exists during HFM fabrication via a liquid-liquid demixing process. Numerous parameters including the dope, bore, and outer coagulant chemistries and compositions significantly influence the HFM morphologies produced. In addition, PBI's unique macromolecular characteristics make it a highly challenging polymer for developing asymmetric membranes with controlled morphology. PBI has a rigid rod like molecular structure with extensive H-bonding between molecular chains and π-π stacking, which limits its dissolution in common organic solvents and often results in brittle HFMs.

The challenge of PBI HFM fabrication has been previously pursued towards the goal of further understanding the commercial potential of this exciting materials class. PBI HFM fabrication using ethylene glycol/water, DMAc/water as bore fluid and water as an external coagulant has been reported in the literature for nanofiltration applications [4, 12]. These PBI HFMs exhibited macrovoids and were very brittle after drying, making their fabrication into self-standing membrane and modules a significant challenge [13]. The inferior dry state mechanical properties also presents a major limitation for their application in dry environments such as those encountered in many gas separation applications. Blends of polyimide and polyetherimide with PBI have also been employed with the goal of combining the advantageous properties of each material to create a superior membrane for pervaporation and gas separation [14, 15]. Unfortunately, the exceptional chemical and thermal stability of the neat PBI materials was consistently compromised due to its blending with polymers having relatively weak thermo-chemical properties.

Kumbharkar et al. evaluated PBI HFMs for H_2/CO_2 separation at elevated temperatures [16]. The PBI HFMs were fabricated using DMAc/water as bore fluid and water as external coagulant. The developed PBI HFMs demonstrated a commercially attractive H_2/CO_2 selectivity of approximately 22 at 300 °C. However, the achieved H_2 permeance of approximately 1 GPU at 300 °C is too low for commercial application. Therefore, developing a comprehensive understanding of the PBI phase inversion process to fabricate high performance HFMs having thin selective layer is highly desirable.

The phase inversion based membrane fabrication processes are highly dependent on the polymeric material used and its specific interactions with solvents mandating that each polymer be studied independently. PBI with its rigid straight chain molecular conformation and extensive h-bonding, falls into a distinct class of polymeric materials not widely studied for its liquid-liquid demixing characteristics, particularly those relevant to HFM fabrication. For these reasons, a systematic fundamental study is conducted here to further understand PBI phase inversion characteristics. Specifically, in this work, a systematic study of PBI's phase inversion character is conducted by varying solvent/non-solvent systems to understand their influence on the formation of PBI HFMs. To aid in non-solvent selection, PBI asymmetric films and solid fibers are fabricated and characterized. The influence of bore fluid and coagulant chemistries and compositions on PBI HFM microstructure is also investigated. To further optimize PBI HFM morphology, the polymer dope solution composition is fine-tuned. The developed PBI HFMs are evaluated for their H_2 and CO_2 permeance at 250 °C to benchmark their performance for syngas separation application.

2 Experimental

2.1 Materials

A 26 wt% poly(2,2'-(m-phenylene)-5,5'-bibenzimidazole) (PBI) solution in N,N-dimethylacetamide (DMAc) containing 1.5 wt% lithium chloride as a phase stabilizer (PBI Performance Products Inc., Charlotte, NC) was used as a base polymer dope solution for asymmetric film, solid fiber, and HFM fabrication. DMAc and NMP (N-methyl-2-pyrrolidone) solvents were procured from Acros Organics Inc. (99+%, extra dry) and used as received. Acetone (Alfa Aesar Inc., HPLC grade), methanol (Fischer Scientific Inc., HPLC grade), hexane (Acros Organics Inc., 99+%), ethyl acetate (Fischer Scientific Inc., HPLC grade), ethanol (Fischer Scientific Inc., anhydrous), isopropanol (Acros Organics Inc., ACS plus grade), butyl acetate (Sigma Aldrich Inc., 99+%), and xylene (Fischer Scientific Inc., ACS grade) were used as coagulants. Deionized (DI) water used in all experiments was produced by a Barnstead™ E-Pure™ system (Thermo Fischer Scientific Inc.) with a resistivity of 18 MΩcm.

2.2 Viscosity Measurement

The dope solution viscosity was measured using a Brookfield Model DV-II+ viscometer with a SC4-34 spindle. The temperature range for viscosity measurements was from 25 to 75 °C, which was controlled using a water jacketed cell.

2.3 Non-solvent Selection

The non-solvent screening for PBI phase inversion was conducted via asymmetric film and solid fiber fabrication. Initially, the commercially available polymer dope solution (PBI/DMAc/LiCl (26/72.5/1.5 wt%), hereafter referred to as the "commercial dope") was selected for use in these studies. However, due to its high viscosity, good quality asymmetric films were not able to be consistently fabricated from this dope composition. Instead, this solution was diluted to a lower polymer concentration (PBI/DMAc/LiCl (19.6/79.3/1.1 wt%)) for asymmetric film fabrication. The PBI asymmetric films were fabricated by casting polymer solution onto a glass slide using an adjustable thickness Baker film applicator. Solid symmetric fibers were fabricated from the commercial dope solution by flowing the dope solution through a simplified spinnerette comprising of a small bore stainless steel tubing (outer diameter = 1600 µm and inner diameter = 350µm) using a high pressure syringe pump (Model 260D, Teledyne Isco Inc.).

2.4 HFM Fabrication

PBI HFMs were fabricated using solution spinning via a non-solvent induced phase inversion process. The dope solution was diluted by adding DMAc and mixed and degassed using a high speed centrifugal mixer (AR-250, Thinky Inc.) prior to use. The degassed dope was transferred into a syringe pump (Model 260D, Teledyne Isco Inc.) while the bore fluid of desired composition was transferred into another syringe pump (Model 100DM, Teledyne Isco Inc.). The dope and bore fluids were passed through the annulus and inner tube of a tube-in-orifice spinneret, respectively, during the spinning process. The nascent hollow fiber was allowed to fall freely into an external coagulation bath without any air gap. The formed fibers were immersed in DI water for 24 h to remove residual solvent followed by sequential solvent exchange prior to drying. For sequential solvent exchange, the fibers were immersed in acetone for 12 h followed by hexane for 12 h and later dried in ambient air. All processes including the drying were conducted at ambient temperature.

2.5 Morphological Study

The morphology of the PBI HFMs was investigated using scanning electron microscopy (SEM). The HFMs were fractured in liquid nitrogen and coated with a 10 nm gold/palladium conducting layer using a precision etching coating system (Model 682, Gatan Inc.). Both the surface and cross-sectional images were obtained using a Field Emission Gun SEM (Inspect F, FEI Company Inc.).

2.6 Module Fabrication and Gas Permeation Measurement

HFM evaluation at elevated temperatures requires leak-free installation in a membrane test cell with the ability to withstand high temperatures (ca. 250 °C). PBI has good adhesion properties to stainless steel at high temperature, therefore the commercial (26wt.%) dope solution was used as a potting/sealing material for laboratory scale single fiber module fabrication. The PBI HFMs tested in this work were approximately 8 cm long. An approximately 3 cm long stainless steel hypodermic tube was partially inserted into one end of the HFM and PBI dope was applied overlapping the contact area between the hypodermic tube and fiber. The other end of the membrane module was sealed (i.e. dead-ended) using a drop of the PBI dope. The membrane was dried in an inert environment at room temperature overnight followed by drying at 105 °C in air to remove the residual DMAc. After drying, the PBI HFM was installed in a stainless steel membrane housing assembly using a standard chromatographic fitting with graphite ferrule for a gas-tight connection with the hypodermic tube.

Pure H_2, CO_2, and N_2 permeation experiments were performed using a constant-volume/variable-pressure method. A feed pressure of approximately 20 psia and a module temperature of 250 °C were used for all experiments. The upstream and downstream pressures were measured using high accuracy pressure transducers (MKS Instruments Inc., ±0.25% FS). The permeation rate was calculated from the slope of the linear part of the permeate pressure rise versus time curve using Equation (1).

$$\text{Permeance, P} = \frac{\mathrm{dp}}{\mathrm{dt}}\left(\frac{\mathrm{VT_0}}{\mathrm{P_0 T \Delta p A}}\right) \tag{1}$$

where, dp/dt is the pressure rise; V is the downstream volume; Δp is the pressure difference between membrane upstream and downstream side; T_0 and P_0 are the standard temperature and pressure, respectively, and A is the effective membrane surface area. The ideal selectivity for a gas pair is calculated using the ratio of their gas permeances.

3 Theoretical Approach

HFMs for gas separation application require an asymmetric structure - a thin, dense skin as a selective layer at the outer membrane surface and a highly porous sub-structure to provide mechanical support. For practical use, the thickness of the dense skin should be as thin as possible to achieve a high permeance. On the other hand, to achieve high selectivity, one must minimize defects in the selective layer. The support layer should be macro-void free because the macro-voids are weak points leading to the HFM failure under high differential pressures. These characteristics are especially important for elevated temperature operations. The HFM morphology is controlled by optimizing the chemistry and composition of the bore fluid and coagulant. Overarchingly, the bore fluid controls the HFM's inner side morphology, largely the support structure, and the coagulant controls the outer side of the fiber and the selective layer. In general, HFM fabrication in a delayed demixing region of the polymer/solvent/non-solvent phase diagram is preferred to maximize fiber morphology control and to realize a uniform, open cellular support structure. To spin fibers in a continuous and commercially viable mode, a fast exchange rate is preferred to minimize coagulation time. Thus, the production of hollow fibers with desirable morphological characteristics at an acceptable formation rate involves controlling the solvent/non-solvent interactions with the dope solution.

During a HFM formation via phase inversion processes, many variables, such as dope, bore and outer coagulant (i.e. non-solvent) composition, solvent/non-solvent exchange rate, solvent and non-solvent solubility parameters, dope, bore, and coagulant temperatures, and post-treatment conditions, determine the morphology of the final polymer membrane. Out of these variables, the chemistries and compositions of the bore and outer coagulant are the most vital parameters. The mass transfer rate and nature of diffusion between non-solvent and solvent dictate the ultimate microstructure of the formed HFM. The exchange rate between solvent and non-solvent is largely dominated by diffusion, with the exchange rate being directly proportional to the diffusivities of solvent and non-solvent. The difference in the solubility parameters of the solvent and non-solvent also affect the exchange rate while altering the solubility of the polymer in the transient polymer/solvent/non-solvent mixture leading to delayed or instantaneous demixing. Therefore, the non-solvent selection for tailoring the phase separation of the polymer solution is critical.

3.1 Solvent/Non-Solvent Solubility Parameters

The solubility parameters of non-solvents and DMAc will affect the solubility of PBI in the mixture of DMAc and the non-solvent during the non-equilibrium state of phase inversion process. The solubility parameters can be calculated from cohesive energies of a solution. The cohesive energy per unit volume is the energy necessary to remove a molecule from its neighboring molecules, as in the case of evaporation. The solubility (Hildebrand) parameter δ is the square root of the cohesive energy. Since the intermolecular forces are determined by the sum of secondary forces (dispersion force, polar force and hydrogen bonding), a more useful way to define a suitable solvent for a polymer is to divide the solubility parameter into three parts: 1) δ_d, the contribution of dispersion force; 2) δ_p, the contribution of the polar force; and 3) δ_h the contribution of H-bonding. These three solubility components are called the Hansen parameters. The relation between the Hansen parameters and Hildebrand parameter is given in Equation (2).

$$\delta^2 = \delta_d^2 + \delta_p^2 + \delta_h^2 \tag{2}$$

$$\Delta\delta_{S-P} = \left[\left(\delta_{d,s} - \delta_{d,p}\right)^2 + \left(\delta_{p,s} - \delta_{p,p}\right)^2 + \left(\delta_{h,s} - \delta_{h,p}\right)^2\right]^{0.5} \tag{3}$$

From thermodynamic considerations and experimental observations, δ_d and δ_p are closely related, while the effect of δ_h is quite different. Therefore, the parameter $\delta_v = (\delta_d + \delta_p)^{1/2}$ is often plotted against δ_h to compare various polymer/solvent combinations. For a given polymer, based on the $\Delta\delta_{(P\text{-}S)}$ values calculated using Equation (3) between polymer and solvents, the "solubility circle" associated with this polymer is determined. Typically, when the $\Delta\delta_{(P\text{-}S)}$ value is less than 5, this solvent is referred to as a "good" solvent, and will dissolve and/or swell the polymer [17]. In the same way, the difference in the solubility parameters of two solvents also determines their miscibility. The smaller the value of $\Delta\delta_{(S1\text{-}S2)}$ is, the better the solvent 1 and solvent 2 miscibility. The solubility parameters of the nine solvents, DMAc, and PBI are given in Table 1 [17, 18]. The plot of δ_v and δ_h for DMAc and the solvents is shown in Figure 1. The green "solubility circle" indicates potentially good solvents or co-solvents for PBI. Among these solvents, DMAc and acetone are potentially good solvents or co-solvents for PBI based on their Hansen solvent parameters. In reality, PBI is only partially soluble at ambient conditions in a few aprotic solvents (e.g. DMAc, NMP) and is not soluble in acetone [19]. Since DMAc has high boiling point and is an attractive solvent for industrial settings, it is widely used as a common solvent for many applications including those served by the commercial PBI dope product. Among these nine solvents acetone, EA, and BA, grouped as weak polar solvents, are near/within the circle; thus, a delayed demixing is expected when they are used as coagulants (also called non-solvent). On the other hand, since water and alcohols, grouped as polar solvents, are far away from this circle, instant demixing is expected when they are used as coagulants. Hexane and xylene, grouped as non-polar solvents, sit between the two aforementioned groups, the demixing process is expected to sit between these two groups.

Table 1: The solubility parameters of non-solvent, DMAc, and PBI.*

Chemical compound	**δ_h $(J/cm^3)^{1/2}$**	**δ_p $(J/cm^3)^{1/2}$**	**δ_d $(J/cm^3)^{1/2}$**	**δ $(J/cm^3)^{1/2}$**	**$\Delta\delta_{(P-S)}$ $(J/cm^3)^{1/2}$**
Non-solvents					
Water	34.2	31.1	13.3	48.2	34.2
Methanol (MeOH)	22.3	12.3	15.2	29.7	14.0
Ethanol (EtOH)	19.5	8.8	15.8	26.6	10.7
Isopropyl alcohol (IPA)	16.4	6.1	15.8	23.6	8.1
Isobutyl alcohol (IBA)	17.0	5.7	15.2	23.5	8.9
Acetone	7.0	10.4	15.5	19.4	3.1
Ethyl acetate (EA)	9.2	5.3	15.2	18.6	4.0
Butyl acetate (BA)	6.4	3.7	15.7	17.4	5.8
Xylene	1.2	0.8	17.2	17.3	11.0
Hexane	0	0	14.8	14.8	12.7
Solvent:					
DMAc	10.2	11.5	16.8	22.8	3.1
Polymer:					
PBI:	8.9±2.5	8.7±3.8	17.3±1.0	21.7±2.0	

* Solubility parameters of solvents and PBI are obtained from reference [17] and [18]

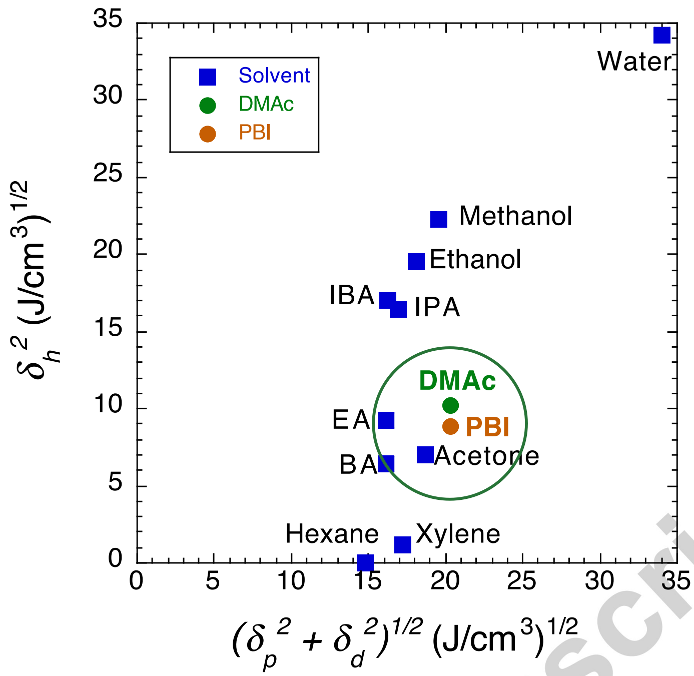

Figure 1: A plot of δ_v and δ_h - solubility parameters of non-solvents, DMAc and PBI.

3.2 Solvent/Non-Solvent Diffusion

Predicting how a given solvent/non-solvent pair interacts during HFM formation is difficult because the phase inversion process is a non-equilibrium process that is influenced by both thermodynamic and kinetic parameters. To conceptually capture this complicated process, we have employed a simplified approach to study the mass transport processes during the demixing process of the PBI/DMAc dope solution and coagulant. As a first approximation, we focused on the initial demixing process between the dope and coagulant. We assumed that during the very early contact stage, the diffusion only occurs at the interface between DMAc in the dope and non-solvent, therefore the system could be considered as a dilute binary. In this case, the diffusivities of DMAc in non-solvent (D_1) and the non-solvent in solvent (DMAc) (D_2) can be theoretically derived. This estimation provides insight into the kinetic aspects of the phase inversion process, i.e., the exchange rate between DMAc and non-solvent.

For dilute non-electrolyte solutions, Equation (4) is used to calculate the diffusivity in an organic solvent [20] and Equation (5) for diffusivity in an aqueous solution .

$$\frac{D^{o}_{AB}\mu_B}{T} = 8.52 \times 10^{-8} V_{bB}^{-1/3}\left[1.4\left(\frac{V_{bB}}{V_{bA}}\right)^{1/3} + \frac{V_{bB}}{V_{bA}}\right] \quad (4)$$

$$D^{o}_{AB} = \frac{13.26\times10^{-5}}{\mu_{wT}^{1.4} V_{bA}^{0.589}} \quad (5)$$

where, D°_{AB} is the diffusivity of molecule A in solvent B (cm^2/sec), μ_B is the solvent viscosity (cP), μ_{wT} is viscosity of water at T (cP), T is the temperature (K), and V_{bA} and V_{bB} are the molar volumes of molecule A and molecule B at their normal boiling temperature (cm^3/gm-mole). Clearly both the solvent/non-solvent viscosity and molar volume determine the diffusivity of molecule A in molecule B. For a non-solvent with low viscosity and small molar volume, DMAc will have a high diffusivity. Likewise, a non-solvent with small molar volume will diffuse faster in DMAc than those non-solvents with high molar volumes.

We have selected a series of “model” non-solvents to present here for illustration purposes. These non-solvents include water and a series of common organic solvents with varied polarity. While the “optimum” coagulant system for the asymmetric PBI membrane formation will likely comprise mixtures, the evaluations on relatively simple systems presented here illustrate the various components and methods included in our selection/down-selection processes, and also provided the basis for defining our advanced coagulant systems. The properties of these non-solvents and DMAc are listed in Table 2.

Table 2: The physical properties of model non-solvents and DMAc.

Compound	Molecular weight (gm/mole)	Boiling point (°C)	μ_B at 25 °C (cP)	V_b (cm^3/gm-mole)
Non-solvent:				
Hexane	86.18	68.8	0.29	140.6
Xylene	106.16	138-144	~0.7	~145.0
Acetone	58.08	57	0.32	77.7
Ethyl Acetate (EA)	88.11	77	0.44	106.3
Butyl Acetate (BA)	116.16	125	0.69	152.2
Water	18	100	0.89	19.4
Methanol (MeOH)	32.04	65	0.55	43.4
Ethanol (EtOH)	46.07	78.5	1.08	62.8
Isopropyl alcohol (IPA)	60.10	82	2.01	83.1
Isobutyl alcohol (IBA)	74.12	107	3.34	101.8
Solvent:				
DMAc	87.12	166	0.92	101.5

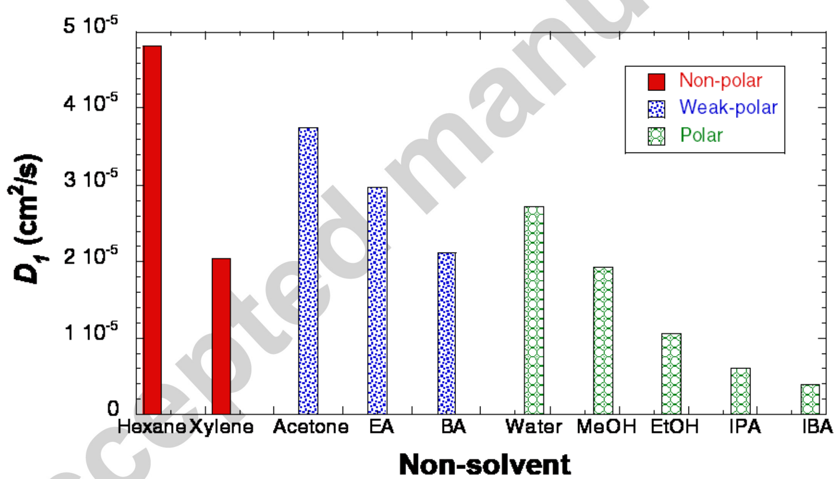

Figure 2: Diffusivity (D_1) of DMAc in non-solvents at 25 °C. The acronyms used for solvents are provided in Table 2.

The diffusivity (D_1) of DMAc in various organic solvents and water is calculated using Equations (4) and (5). The results are presented in Figure 2. The non-solvents are divided into three categories – non-polar, weak-polar, and polar solvents. The polar non-solvents assessed have high viscosities, thus, the diffusivity of DMAc in this group of non-solvents is relatively slow. This effect is especially true for both IPA and IBA. Water is exceptional because of its exceptionally small molar volume. Hence, DMAc diffuses at the highest rate in water for the polar group. For the weak-polar non-solvents, which have large molar volumes but low viscosities, DMAc diffuses at a relatively fast rate on average compared to the other two groups. Among all of these non-solvents, hexane (non-polar) has the lowest viscosity, which allows DMAc to diffuse into it at the highest rate.

During the coagulation process, when the dope solution and non-solvent contact, the non-solvent will diffuse into the PBI/DMAc domain as well. Using Equation 4, we also calculate the diffusivity (D_2) of each non-solvent in DMAc. The results are presented in Figure 3. Since water has the smallest molar volume, it diffuses into DMAc at the fastest rate. Conversely, butyl acetate (BA) has the largest molar volume and thus, will diffuse into DMAc at the slowest rate. Overall, the polar group has higher diffusivities than the other two groups, which is opposite to the DMAc diffusivity into the non-solvent, as shown in Figure 2.

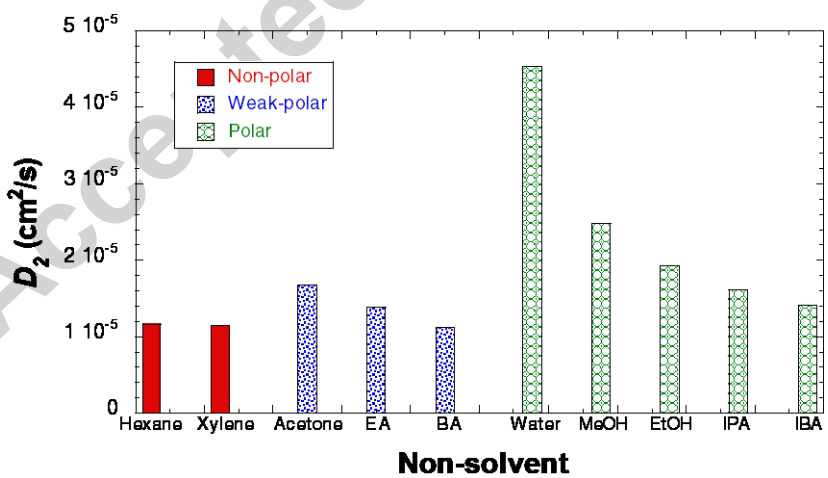

Figure 3: Diffusivity (D_2) of non-solvent in DMAc at 25 °C. The acronyms used for solvents are provided in Table 1.

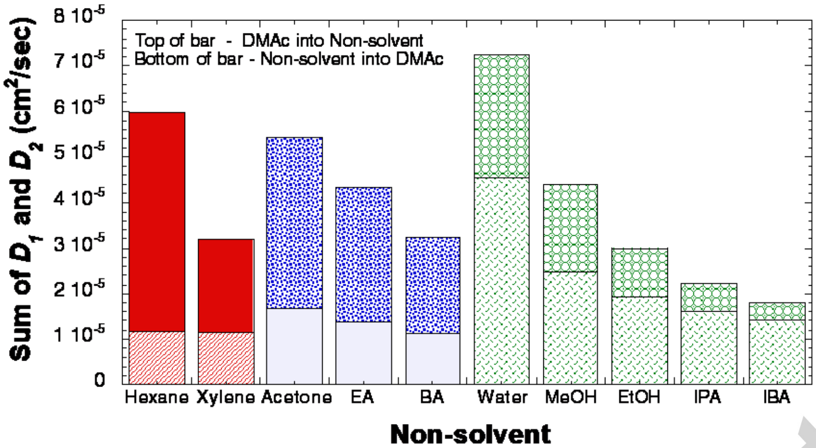

Figure 4: The sum of D_1 and D_2 for each DMAc/non-solvent pair at 25 °C.

Since it is the combination of these diffusion events that ultimately dictates the exchange rate between DMAc and the non-solvent, the mass transfer rates in both directions must be considered to refine non-solvent selection. The sum of D_1 and D_2 for each non-solvent/DMAc pairing is presented in Figure 4. For the polar group, the exchange rate between DMAc and water is the fastest. As water has the highest diffusivity into DMAc, the precipitation of PBI in the water bath is likely controlled by the counter-diffusion of water into the polymer solution domain. Correspondingly, precipitation via a water bath typically results in instantaneous de-mixing. As the molecular chain length and size (water<methanol<ethanol<IPA<IBA) of the polar non-solvents increases, counter-diffusion of the non-solvent in DMAc decreases. Additionally, the increased molecular volume of the alcohols also results in a higher viscosity and thus, a decrease in the diffusivity of DMAc into the alcohols. These combined influences are anticipated to lead to an overarching reduction/slowing of the exchange rate and a corresponding observed transition in the precipitation behavior from an instantaneous de-mixing to a delayed de-mixing. Accordingly, the morphology of the membrane changes from less uniform (including marcovoids) to more uniform porous microstructure [21]. For the other two

groups, a fast exchange rate is expected for hexane in the non-polar group and acetone in the weak polar group. However, the largest contributor in providing fast exchange in the case of hexane and acetone is DMAc diffusion in the non-solvent. In contrast, in the cases of polar solvents as coagulants, the large combined rate is derived from a high non-solvent diffusion in DMAc. In summary, the combined effects of the diffusion process and the miscibility between solvent and non-solvent determines the morphology of the PBI membranes formed through the phase inversion processes.

4 Results & Discussions

4.1 Viscosity Influences

Viscosity of the dope is a key parameter in defining the phase inversion kinetics, which ultimately affect membrane microstructure and separation performance. The viscosities of the diluted dope solutions as a function of composition and temperature (25 to 75 °C) are presented in Figure 5. For all dope compositions, the viscosity decreases exponentially with increasing temperature. In addition to the viscosity of the dope solution, the polymer concentration strongly affects the phase inversion process and thus, the morphology of the final membrane. Therefore, these variables provide an opportunity to tune the phase inversion characteristics of the HFM fabrication process.

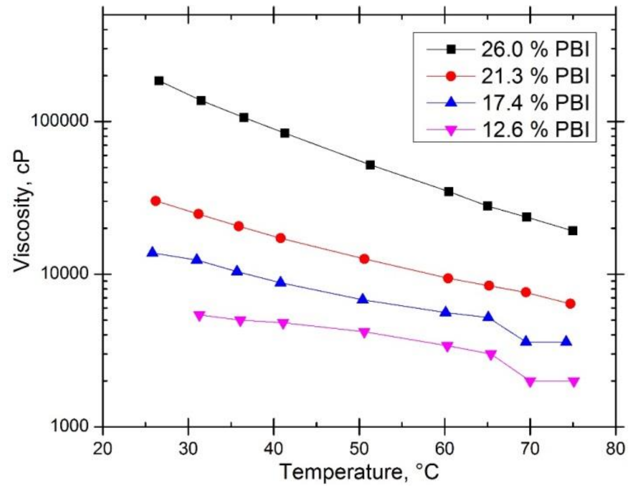

Figure 5: The effect of temperature on the viscosity of PBI/LiCl/DMAc solution

4.2 Non-Solvent Selection

The formation of desirable PBI membrane microstructures is highly challenging due PBI's complex chemical properties. Although the comparison study of the solubility parameters of PBI and solvents provides insight into their compatibility, the true suitability of each of the non-solvents from Table 1 for use in PBI phase inversion is verified by fabricating and characterizing asymmetric films and solid fibers from those non-solvents. The SEM images of PBI membranes prepared using a PBI/LiCl/DMAc (19.6/1.1/79.3 wt.%)) solution and a set of non-solvents are presented in Figure 6. The results of this initial screening are summarized below.

- Highly porous membranes are obtained for acetone, methanol, ethanol and isopropanol.
- Dense membranes with closed cellular structure are observed for hexane, ethyl acetate, water, toluene, butyl acetate and xylene.

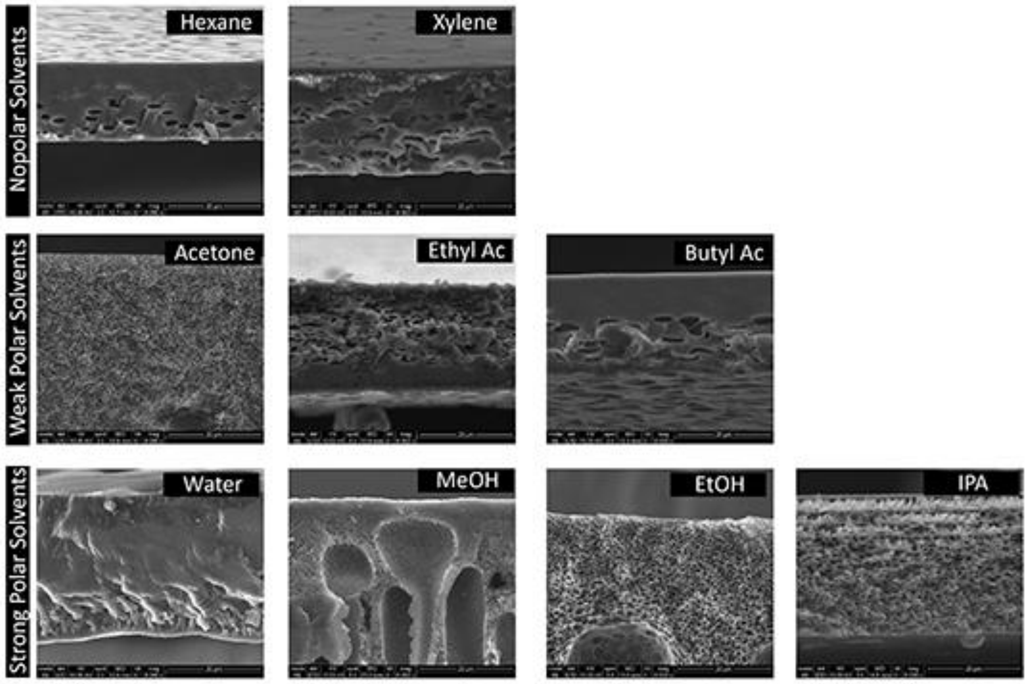

Figure 6: SEM micrographs of asymmetric PBI films prepared using 19.6 wt% PBI dope in nonpolar, weak polar and polar solvents as coagulants.

The formation of these two highly distinct microstructures is overarchingly explained by the diffusion characteristics of the non-solvent into the dope solution and vice versa. In general, porous structures indicate that the non-solvent diffusion into the PBI dope solution is much faster than the DMAc outward diffusion into the coagulant. Conversely, dense structure formation is predominantly due to the faster DMAc outward diffusion from the dope solution compared to the coagulant inward diffusion. For the polar group consisting of methanol, ethanol and isopropanol, the diffusivities D_1 and D_2 are equipotential, indicating formation of porous structures. Water, which is also part of polar group, presents an exception to this correlation and observation. This exception is likely function of several factors including a difference in the actual water diffusivity in the PBI dope as compared to that calculated from pure DMAc. A strong interaction of H_2O with the N-H functionality of PBI is also anticipated to have a substantial influence on the phase inversion dynamics. In the case of the weak polar group, the sum of the two diffusivities (D_1+D_2) is highest for acetone, which is likely responsible for the porous structure formation. Furthermore, the small value of $\Delta\delta_{(P\text{-}S)}$ (Section 3.1) between PBI and acetone suggests that acetone is a good solvent for PBI as well, which causes delayed demixing when the PBI/DMAc dope solution is immersed inside the acetone bath. The delayed demixing not only allows acetone to penetrate deeply inside the dope solution, but also significantly slow down the phase inversion process. As a result, the membrane with a uniform porous distribution is obtained.

The influence of non-solvents on the asymmetric PBI film formation discussed above indicate that some non-solvents are attractive for porous microstructure formation, which is a desired microstructure for the membrane sub-structure and inner surface layer. Therefore, these non-solvents including, acetone, methanol, ethanol, and isopropanol, were selected for the fabrication of PBI solid fibers (Figure 7). For comparison purpose, solid fibers were also fabricated using water. Similar to the observed morphology of the asymmetric films, solid fibers formed using acetone, methanol and ethanol as coagulant have a very porous morphology. The size of porous/cellular features increased in the following order: methanol<ethanol<acetone. Macrovoids are also evident in the fibers formed using methanol and ethanol. The fiber formed using IPA and water have dense morphologies. In the case of IPA, closed cellular pores are present in much lower fraction than that compared to the porous morphologies produced by smaller alcohols, methanol or ethanol. Overall, the size of cellular features for fibers formed in the alcohols correlate well with their molecular sizes.

Based on the results of initial non-solvent screening discussed above, acetone, methanol, and ethanol are selected for use alone and/or as mixtures during the HFM fabrication as both bore fluid and outer coagulant. Water produced a dense microstructure that will be leveraged for dense selective layer formation. Given the strong impact of water, as observed in the asymmetric film and solid fiber fabrication, coagulant mixtures comprising small quantities of water will also be investigated towards obtaining a cohesive dense selective layer on the outer surface.

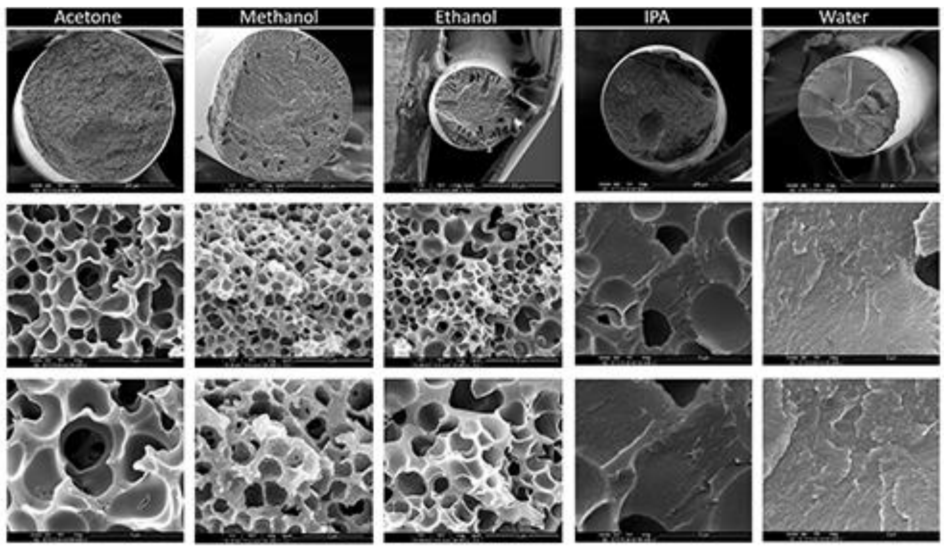

Figure 7: SEM micrographs of asymmetric PBI solid fibers prepared using 26 wt% PBI dope in the selected coagulants.

4.3 Outer Coagulant and Bore Fluid Investigation

The initial binary (dope/non-solvent) screenings discussed above laid the foundation for screening the influences of the ternary (outer coagulant, bore fluid and dope composition) component combinations during HFM fabrication. These influences are discussed in the section below.

For membrane applications, outer surface layer morphologies ranging from porous to dense are desirable depending on the membrane configuration and use. The outer coagulant has a significant influence on the morphology at the HFM exterior surface. To investigate the impact of the down-selected non-solvents on the HFM outer surface morphology, PBI HFMs are prepared using a fixed dope composition (commercial PBI dope (26 wt% polymer)) and a fixed bore fluid composition. For these trials, acetone and water are used as outer coagulants. Acetone is used as a bore fluid with the aim of obtaining a highly porous inner surface.

As expected, porous and dense bulk fiber morphologies are observed for acetone and water, respectively. The HFMs obtained in both scenarios are macro-void free. Acetone forms a dense selective layer with closed cellular structure and porous underlying support structure (Figure 8a), whereas water forms a completely dense structure (Figure 8b). It is well documented that, when solvent diffuses out of the polymer dope solution faster than the non-solvent diffuses into the polymer dope, a dense membrane is formed [22]. Similar solvent/non-solvent diffusion dynamics likely govern PBI HFM fabrication with water as a coagulant resulting in a dense morphology. The water diffusion into the dope is anticipated to be slower than the outward DMAc diffusion into the water coagulant in this scenario due to the high viscosity of the dope solution.

The stark differences in the HFM morphology fabricated using acetone and water as sole coagulants led to idea of a mixed water-acetone coagulant system for HFM fabrication. The fact that water produces a dense morphology when used as the sole coagulant indicates that its use as a minor component of a coagulant mixture might aid in densification of the outer selective layer, in particular, when the co-coagulant tends to impart a porous morphology, e.g. acetone. Therefore, this hypothesis is initially explored via PBI HFM fabrication in an acetone coagulant containing 1 vol.% water. The addition of 1 vol.% water to an acetone coagulant results in distinct outer surface selective layer formation and a porous underlying sub-structure (Figure 8c).

As a result of this exciting result, the concept of adding water as a minor coagulant component is further extended below where the influence of 0 to 2 vol.% water in an acetone coagulant on the PBI HFM morphology is evaluated.

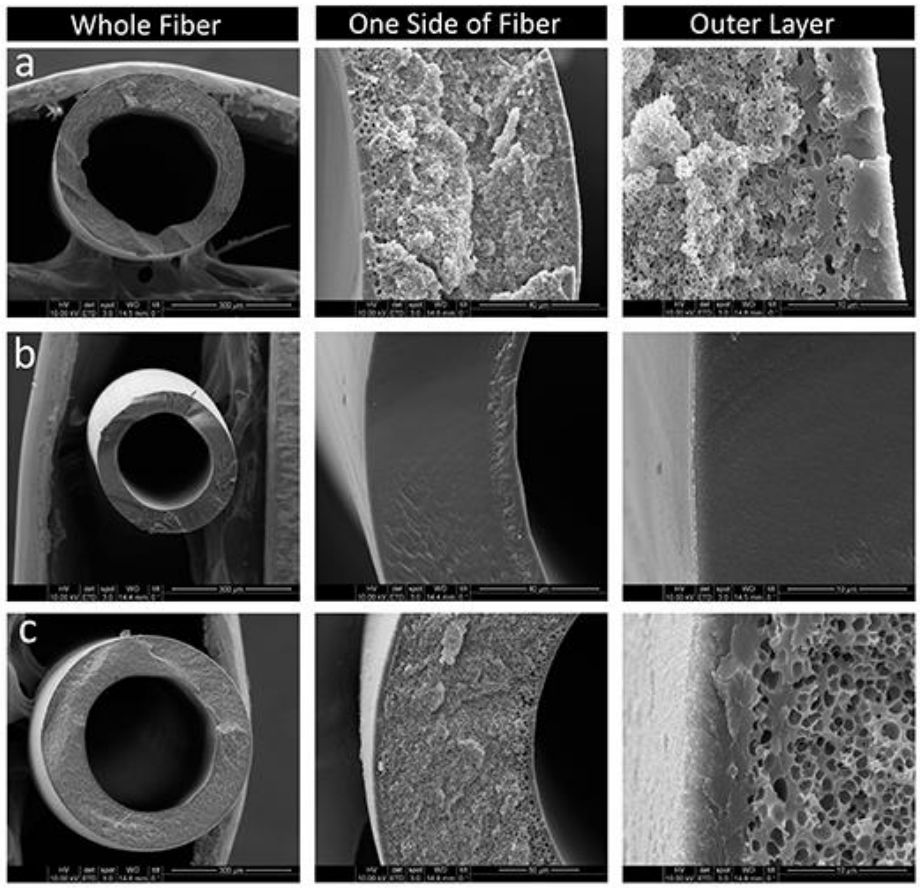

Figure 8: SEM micrographs of PBI HFMs prepared from the commercial PBI solution. Acetone is the bore fluid, and (a) acetone, (b) water, or (c) 1% water in acetone are used as the coagulant.

In a membrane configuration where the feed is on the shell side and permeate is on the bore side, the inner, bore side structure should be highly porous to minimize the gas transport resistance in the fiber. In the asymmetric film and solid fiber fabrication trials, acetone, methanol, and ethanol produced a highly porous structure, as discussed in section 4.2. However, a distinct dense layer at the inner side is observed in HFMs obtained using acetone as the bore fluid (Figure 8a). As discussed in section 4.2, the large influx of non-solvent (acetone) into the polymer solution as compared to DMAc outward diffusion results in porous support morphologies. Based on the solubility parameter analysis for acetone as coagulant a delayed demixing is anticipated (Section 3.1). However, this delayed demixing also results in an increased polymer concentration at the dope solution – bore fluid interface on the inner layer because of DMAc outward diffusion. This increased dope concentration at the inner surface interface is likely responsible for dense layer formation upon solidification [23]. It is anticipated that reducing the demixing time will minimize or eliminate the dope concentration increase at the dope – bore fluid interface resulting in porous inner layer formation. Therefore, methanol and ethanol, which based on solubility parameter analysis should cause an instantaneous demixing, are evaluated as bore fluids with the goal of porous structure formation at the HFM inner surface. SEM micrographs of HFMs prepared using the commercial dope solution and 1% water in acetone as outer coagulant and acetone, methanol and ethanol as bore fluids are presented in Figure 9. Outer integrated dense selective layers are observed in all three types of HFMs. Large finger and hourglass like macro-voids are observed for methanol, whereas relatively small sized macro-voids concentrated on the inner surface are observed for ethanol. The macro-voids are formed due to the instantaneous de-mixing of polymer solution as a result of fast non-solvent/solvent exchange [24]. The extent of macro-voids formation is dependent on the diffusion of non-solvent into the dope solution. The size and density of macro-voids observed in these HFMs correlates well with diffusivity of the non-solvent into DMAc as shown in Figure 3. The diffusivity of methanol into DMAc is higher than that of ethanol and acetone, which is likely a factor influencing the large sized macro-voids formed in the methanol scenario. A thick distinct outer surface layer is formed on the HFMs produced using all three bore fluids.

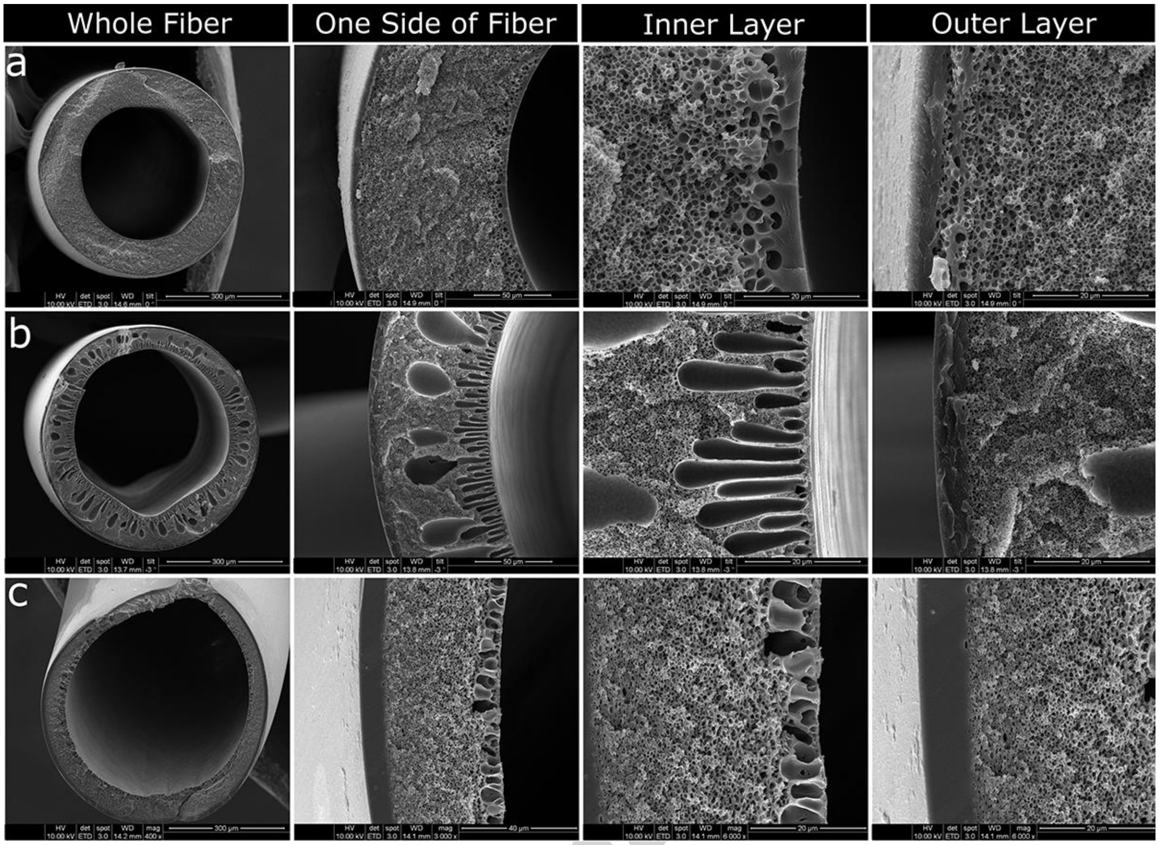

Figure 9: SEM micrographs of PBI HFMs prepared from the commercial PBI dope solution. 1% water in acetone is used as the outer coagulant, and (a) acetone, (b) methanol, and (c) ethanol are used as the bore fluid.

The last phase inversion process parameter studied in the outer coagulant and bore fluid investigation reported in this section is the influence of small water fractions in the coagulant. In this set, PBI HFMs are fabricated using commercial dope, a methanol bore fluid, and coagulants comprising acetone with varied water contents (0-2 vol%). The SEM micrographs of PBI HFMs fabricated using these mixed acetone/water coagulants are presented in Figure 10. The HFMs fabricated using water/acetone mixed coagulants have very similar morphologies indicating that while the presence of water is clearly impactful towards imparting a dense surface layer, the PBI phase inversion process is not significantly impacted by the varied coagulant water content over the evaluated compositional range.

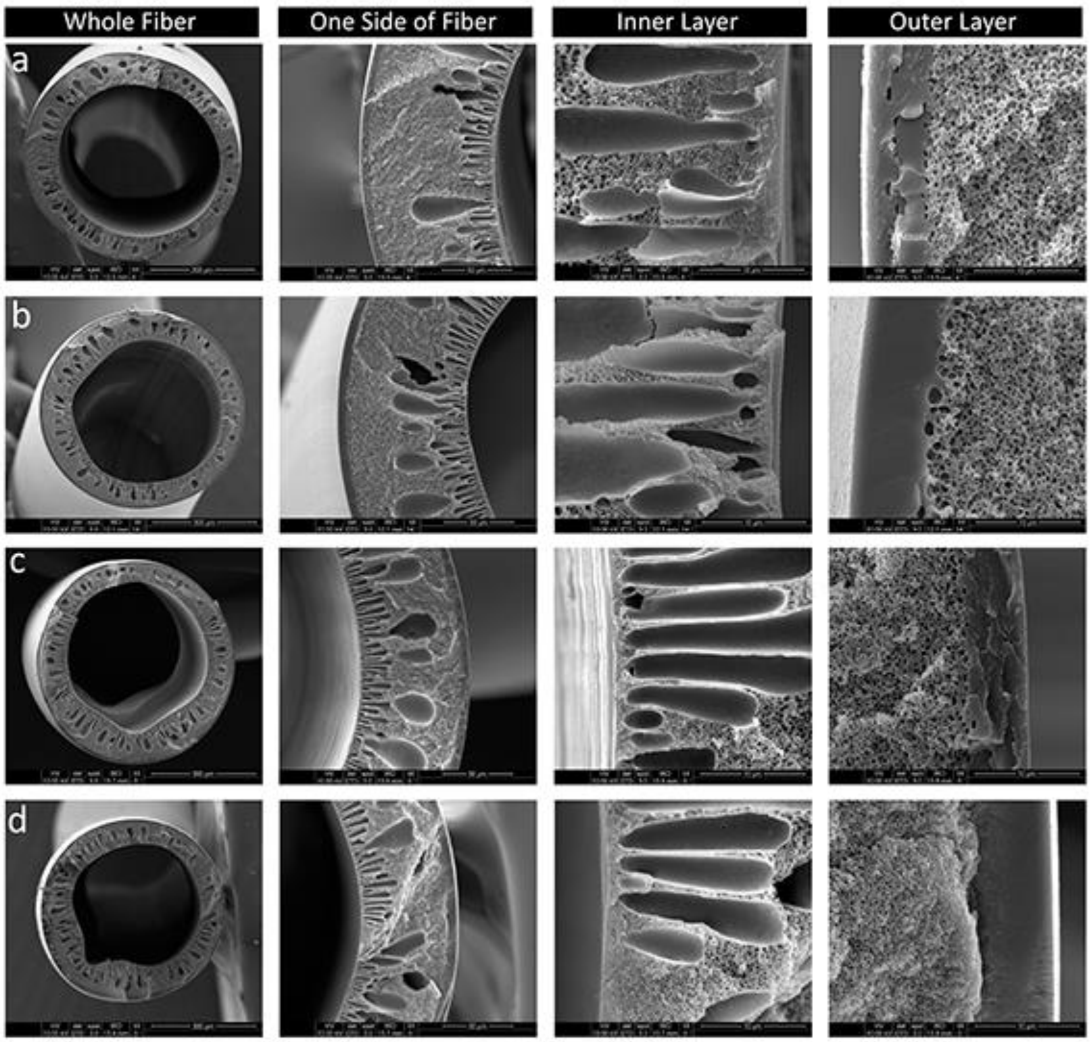

Figure 10: SEM micrographs of PBI HFMs fabricated from the commercial PBI dope solution using methanol as the bore fluid. Acetone with varied water content [a) 0, b) 0.5, c) 1 and 2 vol.%] is used as the coagulant.

4.4 Dope Composition Investigation

Dope solution composition is another parameter that is exploited to further control HFM morphologies. In concert with the bore and coagulant compositions, the dope composition has a significant impact on selective layer thickness and macro-void size and density. The effect of dope composition on the HFM morphology is investigated while holding all other spinning parameters constant.

The morphology of the PBI HFMs fabricated with varied PBI dope concentrations (26.0, 21.3, and 16.5 wt%) are presented in Figure 11. As the PBI concentration reduced from 26 to 21.3 wt%, the support layer porosity is increased, while the selective layer thickness is decreased. A further decrease in the PBI concentration to 16.5 wt% leads to an appreciable amount of macro-void formation from both the inner and outer surfaces and an increase in the overarching HFM porosity. The variation in the morphology of PBI HFMs with the dope composition is attributed to the change in the viscosity of dope, which decreases by an order of magnitude as the PBI concentration is varied from 26 to 17.4 wt% (Figure 5). The dope viscosity is a controlling factor in dictating the relative mass transfer rates between the non-solvent and solvent. The decreased viscosity of the dope solution significantly increases the mass transport of non-solvent in the dope solution domain, which increases the de-mixing process. As a result, large macro-void formation is not observed for 26.0 and 21.3 wt% dope solutions but significantly increases as the polymer concentration decreases from 21.3 to 16.5 wt%. This indicates that a PBI weight fraction near to 21.3 wt% is sufficient to prevent macro-void formation in PBI HFMs. In the subsequent section, the fine-tuning of spinning parameters is discussed with the ultimate goal of preparing PBI HFMs with both an integrated, thin selective layer and a porous support structure.

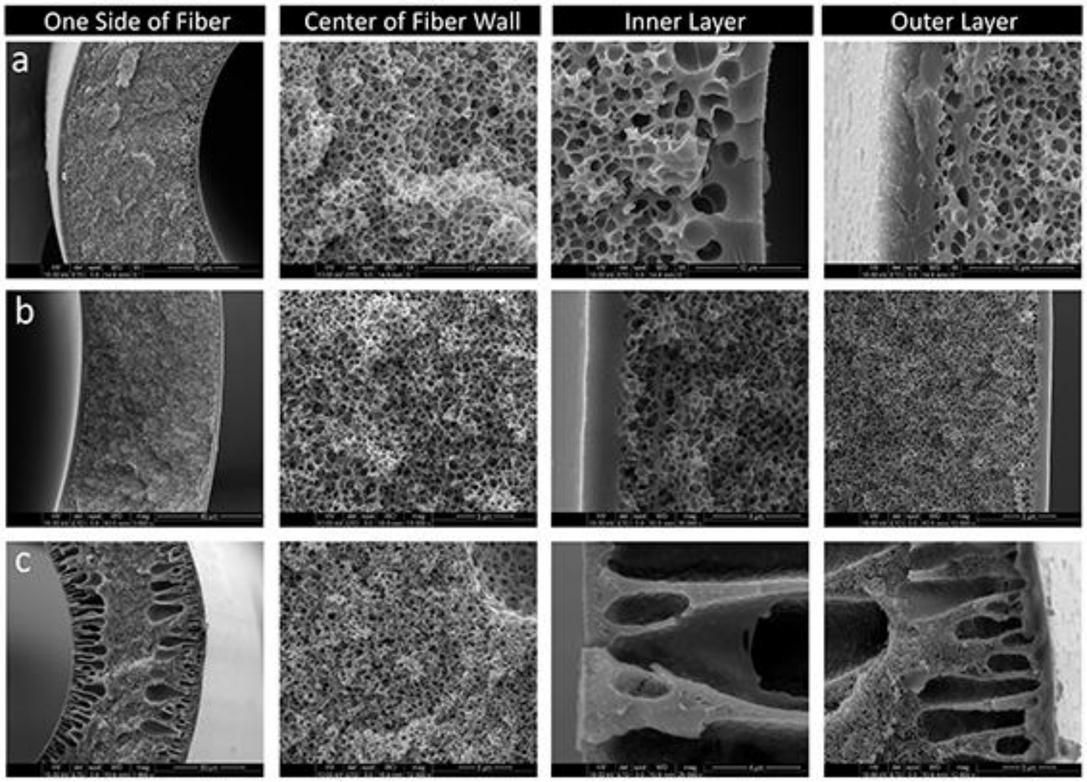

Figure 11: SEM micrographs of PBI HFMs fabricated from (a) 26.0%, (b) 21.3%, and (c) 16.5% PBI dope solutions using acetone as a bore fluid and 1 to 2 % water in acetone as an outer coagulant.

4.5 Selective Layer Optimization and Macro-voids Suppression

A typical industrially attractive asymmetric HFM has a thin selective layer supported by a porous structure where the selective layer is largely responsible for the separation performance of the membrane. Macro-void free PBI HFMs having approximately 1 µm thick dense selective layers both on the inner and outer surfaces are formed for the 21.3 wt% PBI dope, as illustrated in Figure 11b. Such selective layer formation on both inner and outer sides is not desirable as this configuration substantially increases gas mass transport resistance and results in low permeance. Here the objective is to prepare PBI HFMs with a thin selective layer integrated with porous inner surface layer and support structure. To achieve this objective, the bore fluid chemistry is manipulated to obtain porous inner layer characteristics. PBI HFMs fabricated using ethanol and acetone/ethanol as bore fluids are presented in Figure 12. For this set of HFM fabrication conditions, the dope solution is 21.3 wt% PBI and the coagulant is 1 vol.% water in acetone. A highly porous inner surface layer and dense outer surface layer are observed with ethanol as the bore fluid. The use of acetone/ethanol as the bore fluid results in macro-void formation at the inner side for both acetone/ethanol ratios (85/15 and 15/85). The relative diffusivity of ethanol is higher than acetone with respect DMAc, which indicates high mass transfer rate of ethanol into the dope solution results in macro-void formation.

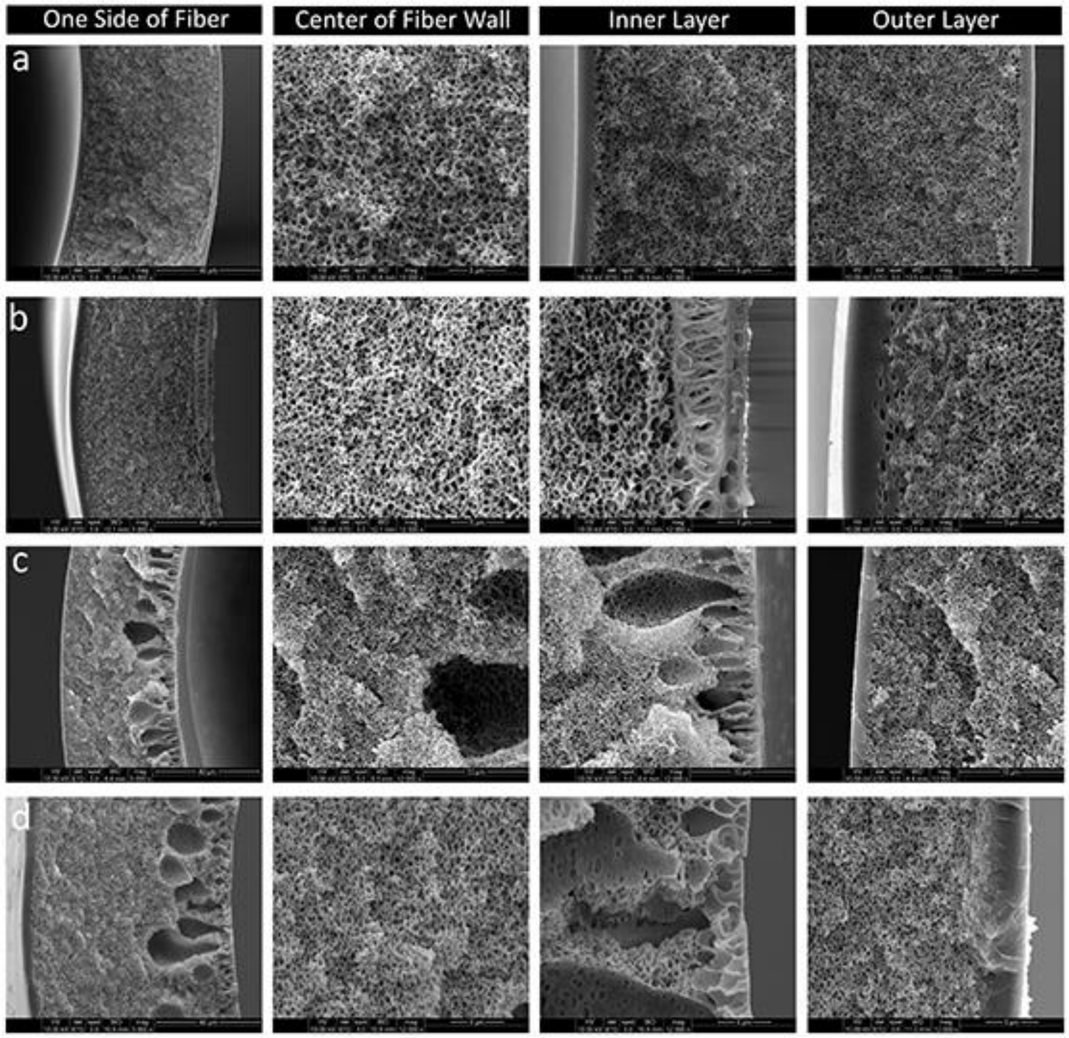

Figure 12: SEM micrographs of HFMs prepared from the 21.3% PBI dope using bore fluids (a) acetone, (b) ethanol, (c) acetone/ethanol (85/15), and acetone/ethanol (15/85). 1 to 2% water in acetone was used as a coagulant.

4.6 Gas separation performance of PBI HFMs

Gas permeation data was obtained on selected PBI HFMs fabricated in this work to understand the influence of the HFM morphology on its gas separation properties. The exact HFM phase inversion fabrication process parameters for the evaluated fibers are provided in Table 3. The SEM images comparing the outer and inner layers of the HFMs are shown in

Figure 13. While the HFMs selected for gas permeation evaluation have a dense selective layer with a thickness of ~2 μm on the outer surface, the inner surface layer morphology of these fibers varied. HFM-1 and HFM-2 also have a distinct dense layer on the inner surface; while HFM-3 appears to have a porous inner surface. HFM-1 is macro-void free while macro-voids are found in HFM-2 and HFM-3.

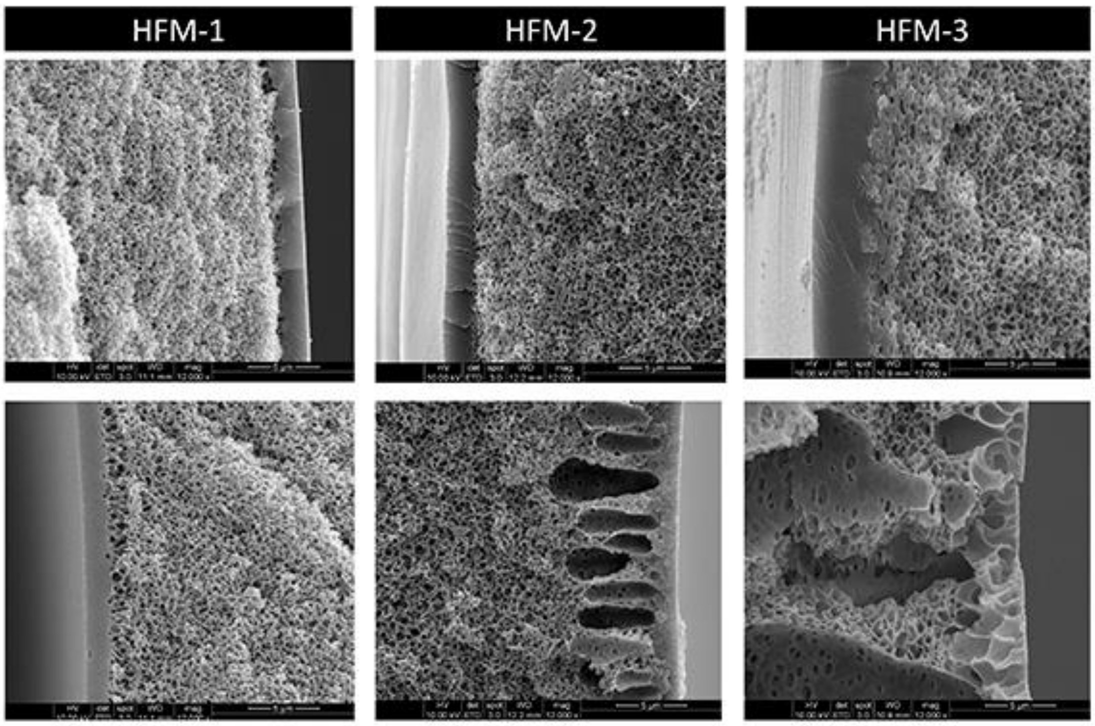

Figure 13: SEM images of the outer and inner layer of PBI HFMs evaluated for gas permeation. Top row: outer surface & bottom row: inner surface.

Table 3: PBI HFM spinning parameters

Spinning Parameters	PBI HFM		
	HFM-1	HFM-2	HFM-3
PBI Composition (wt%)	21.3	20.0	21.5
Bore Fluid	Acetone	Acetone	Acetone/Ethanol (15/85)
Outer Coagulant (% vol.)	0.5% H_2O-Acetone	2% H_2O-Acetone	2% H_2O-Acetone

The ideal gas separation performances of these PBI HFMs measured at 250 °C are provided in Table 4. The H_2 permeance ranges between 7 and 21 gpu while the H_2/CO_2 selectivity varies between 14 and 22.4. The thickness of the HFM effective selective layer from the pure gas H_2 permeability of m-PBI measured at 250 °C is also given in Table 4. The effective thicknesses of all HFMs are much greater than that these determined from the SEM images. This discrepancy likely arises from the presence of dense skin layer on the inner surface and the presence of closed cells in the porous sub-layer. Both factors contribute to an additional mass transfer resistance in the HFM resulting in lower H_2 permeances than that expected from the measured outer selective layer thickness alone.

Table 4: Ideal H_2 permeance and H_2/CO_2 and H_2/N_2 selectivity measured for PBI HFMs at 250 °C. The effective thickness is calculated from H_2 permeability of PBI thin film [19].

PBI HFM	H_2 Permeance, GPU	H_2/CO_2 selectivity	H_2/N_2 selectivity	Effective Thickness, μm	Skin Thickness from SEM, μm
HFM-1	9.72	17.11	24.12	7.9	3.9
HFM-2	21.0	13.99	18.40	3.7	1.9
HFM-3	7.56	22.37	61.97	10	4.6

The gas separation performance of the PBI HFMs can be tailored by further manipulating the phase inversion process. Further reducing the dope concentration and fine tuning the non-solvent/solvent interactions could lead to thinner selective layers and more porous sub-layer structure and inner surface layer.

5 Conclusions

In this work, we have demonstrated that by manipulating the dope and coagulant chemistry and composition, the microstructure of the PBI HFMs is effectively controlled to achieve a thin selective layer with combined macro-void free porous sub-structure. A large number of non-solvents were evaluated using theoretical predictions combined with experiment to develop a more complete understanding of solvent/non-solvent properties on PBI phase inversion dynamics. The polar non-solvents, except for water, result in porous sub-layer structures; whereas, weak-polar and non-polar non-solvents and water result in dense structures. The non-solvents (with exception to water) having similar solvent/non-solvent diffusion and counter diffusion characteristics produced very porous sub-layer structures with macro-voids. Defect free asymmetric PBI HFMs having H_2/CO_2 selectivity exceeding 20 and a H_2 permeance of 8 GPU at 250 °C were successfully fabricated. Developing a more complete understanding of how to optimize the asymmetric PBI HFM liquid-liquid demixing based fabrication process parameters provides an important scientific foundation towards industrial deployment of PBI based membranes and demonstrates the feasibility of utilizing of the PBI HFM to achieve industrially attractive separation performance for the syngas separations.

Acknowledgements

This project supports the U.S. Department of Energy Office of Fossil Energy (FE)/National Energy Technology Laboratory's Carbon Capture Program. The authors gratefully acknowledge the U.S. DOE/NETL Carbon Capture Program for financial support of the project under Field Work Proposal LANL-FE-308-13. The authors acknowledge PBI Performance Products Inc. for their programmatic contributions. Los Alamos National Laboratory is operated by Triad National

Security, LLC for the National Nuclear Security Administration of U.S. Department of Energy under contract 89233218CNA000001

References

[1] J.S. Wainright, J.T. Wang, D. Weng, R.F. Savinell, M. Litt, Acid‐Doped Polybenzimidazoles: A New Polymer Electrolyte, Journal of The Electrochemical Society, 142 (1995) L121-L123.

[2] L.C. Sawyer, R.S. Jones, Observations on the structure of first generation polybenzimidazole reverse osmosis membranes, Journal of Membrane Science, 20 (1984) 147-166.

[3] K.Y. Wang, T.-S. Chung, J.-J. Qin, Polybenzimidazole (PBI) nanofiltration hollow fiber membranes applied in forward osmosis process, J. Membr. Sci., 300 (2007) 6-12.

[4] K. Wang, T. Chung, Fabrication of polybenzimidazole (PBI) nanofiltration hollow fiber membranes for removal of chromate, Journal of Membrane Science, 281 (2006) 307-315.

[5] I.B. Valtcheva, S.C. Kumbharkar, J.F. Kim, Y. Bhole, A.G. Livingston, Beyond polyimide: Crosslinked polybenzimidazole membranes for organic solvent nanofiltration (OSN) in harsh environments, Journal of Membrane Science, 457 (2014) 62-72.

[6] A. Asadi Tashvigh, L. Luo, T.-S. Chung, M. Weber, C. Maletzko, Performance enhancement in organic solvent nanofiltration by double crosslinking technique using sulfonated polyphenylsulfone (sPPSU) and polybenzimidazole (PBI), J. Membr. Sci., 551 (2018) 204-213.

[7] K.A. Berchtold, R.P. Singh, J.S. Young, K.W. Dudeck, Polybenzimidazole composite membranes for high temperature synthesis gas separations, J. Membr. Sci., 415-416 (2012) 265-270.

[8] S.C. Kumbharkar, Y. Liu, K. Li, High performance polybenzimidazole based asymmetric hollow fibre membranes for H_2/CO_2 separation, J. Membr. Sci., 375 (2011) 231-240.

[9] G. Krishnan, D. Steele, K. O'Brien, R. Callahan, K. Berchtold, J. Figueroa, Simulation of a Process to Capture CO2 From IGCC Syngas Using a High Temperature PBI Membrane, Energy Procedia, 1 (2009) 4079-4088.

[10] K.C. O'Brien, G. Krishnan, K.A. Berchtold, S. Blum, R. Callahan, W. Johnson, D.-L. Roberts, D. Steele, D. Byard, J. Figueroa, Towards a pilot-scale membrane system for pre-combustion CO_2 separation, Energy Procedia, 1 (2009) 287-294.

[11] D.R. Pesiri, B. Jorgensen, R.C. Dye, Thermal optimization of polybenzimidazole meniscus membranes for the separation of hydrogen, methane, and carbon dioxide, J. Membr. Sci., 218 (2003) 11-18.

[12] K.Y. Wang, T.-S. Chung, Polybenzimidazole nanofiltration hollow fiber for cephalexin separation, AIChE Journal, 52 (2006) 1363-1377.

[13] Y. Wang, M. Gruender, T.S. Chung, Pervaporation dehydration of ethylene glycol through polybenzimidazole (PBI)-based membranes. 1. Membrane fabrication, J. Membr. Sci., 363 (2010) 149-159.

[14] T.-S. Chung, W.F. Guo, Y. Liu, Enhanced Matrimid membranes for pervaporation by homogenous blends with polybenzimidazole (PBI), Journal of Membrane Science, 271 (2006) 221-231.

[15] T.-S. Chung, Z.-L. Xu, Asymmetric hollow fiber membranes prepared from miscible polybenzimidazole and polyetherimide blends, Journal of Membrane Science, 147 (1998) 35-47.

[16] S.C. Kumbharkar, Y. Liu, K. Li, High performance polybenzimidazole based asymmetric hollow fibre membranes for H2/CO2 separation, Journal of Membrane Science, 375 (2011) 231-240.

[17] D.W.v. Krevelen, K.t. Nijenhuis, Properties of Polymers 4th ed., 2009.

[18] D. Plackett, A. Siu, Q. Li, C. Pan, J.O. Jensen, S.F. Nielsen, A.A. Permyakova, N.J. Bjerrum, High-temperature proton exchange membranes based on polybenzimidazole and clay composites for fuel cells, J. Membr. Sci., 383 (2011) 78-87.

[19] X. Li, R.P. Singh, K.W. Dudeck, K.A. Berchtold, B.C. Benicewicz, Influence of polybenzimidazole main chain structure on H_2/CO_2 separation at elevated temperatures, J. Membr. Sci., 461 (2014) 59-68.

[20] M.A. Lusis, C.A. Ratcliff, Diffusion in binary liquid mixtures at infinite dilution, The Canadian Journal of Chemical Engineering, 46 (1968) 385-387.

[21] M. Mulder, Basic Principles of Membrane Technology, 2nd ed., Springer Netherlands, 1996.

[22] H. Strathmann, P. Scheible, R.W. Baker, A rationale for the preparation of Loeb-Sourirajan-type cellulose acetate membranes, Journal of Applied Polymer Science, 15 (1971) 811-828.

[23] C.H. Koops, J.A.M. Nolten, M.H.V. Mulder, C.A. Smolders, Integrally Skinned Polysulfone Hollow Fiber Membranes for Pervaporation, Journal of Applied Polymer Science, 54 (1994) 385-404.

[24] C.A. Smolders, A.J. Reuvers, R.M. Boom, I.M. Wienk, Microstructures in phase-inversion membranes. Part 1. Formation of macrovoids, J. Membr. Sci., 73 (1992) 259-275.

Highlights

- Systematic theoretical and experimental study to identify suitable non-solvent for polybenzimidazole (PBI) phase inversion
- Demonstrated ability to control hollow fiber membrane (HFM) morphology by manipulating non-solvent chemistry
- Asymmetric HFMs having thin dense selective layer and porous support morphology achieved
- PBI HFMs having high H_2/CO_2 selectivity at elevated temperatures reported